THE JOURNAL OF PHYSICAL CHEMISTRY B LETTERS

2005, *109,* 13854−13856
Published on Web 07/06/2005

Optical Control of Coherent Lattice Motions Probed by Femtosecond Electron Diffraction

H. Park, S. Nie, X. Wang, R. Clinite, and J. Cao*

Physics Department and National High Magnetic Field Laboratory, Florida State University, Tallahassee, Florida 32310

Received: May 30, 2005; In Final Form: June 23, 2005

We report the study of laser-induced coherent lattice motions using femtosecond electron diffraction. The oscillations of Bragg peak positions associated with a damped lattice vibration along the surface normal were directly observed in real time and with sub-milli-angstrom spatial resolution. In addition, by using a pair of optical excitation pulses and varying their time delay and relative pulse intensities, we demonstrated the successful control of coherent lattice motions.

Coherent control utilizes classical or quantum interferences to manipulate the electronic and structural responses of atoms, molecules, and crystals. It provides a unique way of driving samples into nonequilibrium states not accessible by conventional means. The most widely used control schemes correlate the involved states with excitation photons, either by adjusting their state properties via manipulating parameters of the excitation optical field[1] or by adjusting the phases of the states by controlling the arrival times of ultrashort optical pulses.[2,3] Specifically, a pulse shaper has been used in the former method to change the field's spectral and temporal characteristics.[1] Optical control of coherent lattice vibrations in crystals using the latter approach has been reported using time-resolved optical spectroscopy to monitor the associated periodic modulation of reflection or transmission signals, thus controlling the coherent phonons indirectly.[4−7]

Recent advances in time-resolved diffraction have provided the capability of direct measurement of the coherent lattice vibrations by monitoring the corresponding diffraction signal change on the picosecond and sub-picosecond time scales.[8−13] Coherent control of acoustic phonons using Bragg peak intensity change recorded with picosecond X-ray diffraction has been demonstrated.[14] Here, we present the optical control of coherent lattice motions in a thin-film aluminum sample probed with femtosecond electron diffraction (FED). Oscillations of Bragg peak positions associated with a damped lattice vibration along the surface normal were directly observed with sub-milli-angstrom spatial resolution. In addition, by using a sequence of excitation pulses, we demonstrated the control of the coherent lattice motions on a time scale of a few picoseconds.

The coherent lattice vibrations were excited by ultrafast heating of the Al film with 50-fs near infrared (790 nm) laser pulses from an amplified Ti:sapphire laser system. The polycrystalline thin-film aluminum samples were prepared by thermal evaporation of Al in a high vacuum on freshly cleaved NaCl single-crystal substrates and then detached and transferred in a solvent to transmission electron microscopy (TEM) grids as free-standing films. A film thickness of 25 ± 5.0 nm was measured with an in situ quartz crystal thickness monitor. After femtosecond photoexcitation, the hot free electrons in the film will reach a nearly uniform transient electronic temperature across the film in approximately 300 fs. This we estimated using one-dimension heat diffusion with typical parameters for Al[15] and an optical absorption depth of 7.4 nm.[16] This ultrafast and near homogeneous electron heating combined with the concurrent heating of the lattice through electron−phonon coupling establishes a new, expanded, equilibrium lattice position, which puts the lattice in a highly stressed state in a time scale shorter than the lattice response time. Under this ultrafast and nearly displacive excitation,[17] a coherent lattice vibration centered at the new equilibrium position was launched in the form of acoustic waves. Since the linear dimension of the excitation laser beam (~1 mm) is much larger than the film thickness, the lattice motion can be assumed as one-dimensional (1-D) along the surface normal direction with open-end boundary conditions (free-standing film). This leads to the creation of a 1-D longitudinal standing sound wave (a breathing motion along the surface normal) in the Al film with a vibration period of $T = 2L/v$, where v is the longitudinal sound velocity of 6420 m/s.[18] This ultrafast heating approach has been widely used to generate coherent acoustic phonons in thin films[19] and nanoparticles.[20−22]

Using FED in a transmission mode, we directly monitor lattice motions by taking snapshots of diffraction patterns at different time delays. To reduce the space−charge broadening, the probe electron pulses contain on average less than 1000 electrons/pulse. Their pulse widths ($\Delta\tau_e$) were measured by a streak camera[11] to be less than 450 fs. We assumed a Gaussian shape and used the equation $\Delta\tau_e = K_s\sqrt{W_{str}^2 - W_{un}^2}$, where K_s (150 fs/pixel) is the streaking speed and W_{str} and W_{un} are the full width at half-maximum (fwhm) of electron beam sizes for streaked and unstreaked pulses, respectively. To reduce the temporal degradation[23] resulting from their finite beam sizes, the pump laser (~1 mm beam size) and probe electron (~300 μm beam size) beams were arranged in a nearly collinear configuration with less than 10° cross-angle. Convoluting the excitation laser pulse width, probe electron pulse width, and temporal degradation gave an overall temporal resolution of approximately 500 fs.[11] In addition, the diffraction patterns

10.1021/jp052857u CCC: $30.25

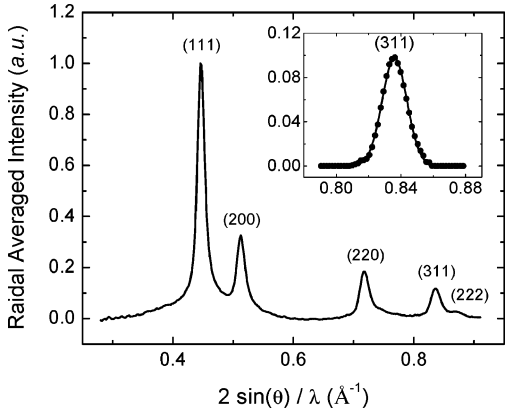

Figure 1. Diffraction intensity curve of free-standing thin-film aluminum. Inset: A typical fit of the (311) Bragg peak to a Gaussian profile. The peak center position was determined to be 0.836 06 ± 0.000 05 Å^{-1} (465.83 ± 0.03 pixels).

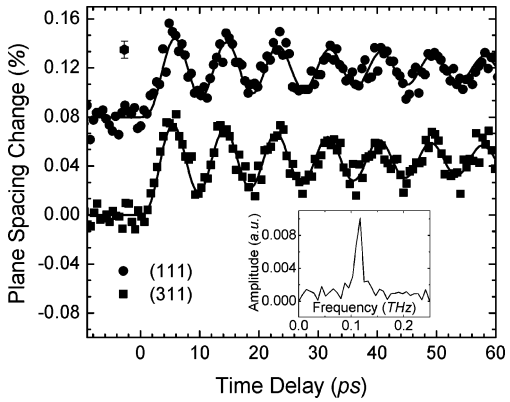

Figure 2. Temporal evolution of the (111) and (311) crystal plane spacing. The time step is 530 fs. Positive time delays correspond to the arrival of probe electron pulses after the excitation laser pulses. The error bar represents one standard deviation in the Gaussian peak profile fitting. The solid curves are fits to the experimental data. Inset: Fourier transform of the temporal evolution of the (311) Bragg peak position. The peak frequency is approximately 0.114 THz, corresponding to a 8.7-ps vibrational period.

without the pump laser were recorded at each time delay and used as a reference for data analysis to correct any extraneous changes, such as probe electron beam walking and the long-term system drift.

A typical diffraction intensity curve of the free-standing thin-film aluminum is shown in Figure 1. This curve is a radial average of the corresponding 2-D diffraction pattern, which was recorded with sub-picosecond electron pulses (<1000 e$^-$/pulse), at a laser excitation fluence of 1.5 mJ/cm^2 and with a probing electron number of approximately 10 million. To obtain a quantitative measurement of the coherent lattice motions, each Bragg peak in an intensity curve was fitted with a Gaussian line profile to determine the peak center (see the inset of Figure 1 for the Bragg (311) peak), which is defined as the peak position. The peak positions obtained with the pump laser on were then normalized to those with the pump beam blocked to eliminate any extraneous errors. This processing scheme, combined with diffraction data of superior signal-to-noise ratio, makes it possible to probe the relative Bragg peak position change with an accuracy of better than 0.02%.

The temporal evolution of (111) and (311) lattice plane spacing as a function of delay times is shown in Figure 2. After optical excitation, the Bragg plane starts an oscillatory motion centered at a newly established and expanded equilibrium lattice position. The vibration has a negative maximum displacement at time zero and displays a nearly cosine time dependence, indicating a displacive excitation mechanism.[17] The solid curves in Figure 2 are fits to the experimental data with a model of damped oscillation.[24] For the (311) data, the oscillatory part gives a vibrational period of 8.7 ± 0.2 ps (~0.115 THz) and a damping time constant of 59 ± 7 ps. The Fourier transform of the (311) peak oscillation is also shown in the inset with a single peak centered at 0.114 THz, which is consistent with the 8.7-ps oscillation period obtained from the fitting. Using a nominal average film thickness (L) of 25 ± 5.0 nm and a sound velocity of 6420 m/s,[18] this 8.7 ps is in good agreement with the vibrational period of a 1-D standing wave $T = 2L/v$.

The temporal evolutions of all the other Bragg peak positions were also analyzed and found to oscillate perfectly in phase with one another with the same vibrational period. This perfect in-phase oscillation supports the model of 1-D breathing vibration of film induced by the nearly uniform heating of the film, which is distinct from the commonly used surface heating excitation approach.[14,19,25] In surface heating, the film thickness is much larger than the light penetration depth, so thermal expansion into the film launches a longitudinal acoustic pulse propagating normal to the plane of the film with many wave vector components, up to the inverse of the optical excitation depth.

For small angle diffraction with a Bragg angle of less than 1.6° in the current experiment, the relative change of linear Bragg peak position (Bragg ring radius $\Delta r/r$) recorded in the diffraction pattern equals the relative change of Bragg angle ($\Delta\theta/\theta$), which in turn equals the relative change of lattice plane spacing ($\Delta d/d$) according to Bragg's law, that is, $\Delta r/r \approx \Delta\theta/\theta \approx \Delta d/d$. Therefore, the relative change of Bragg peak position ($\Delta r/r$) recorded in the diffraction pattern gives a direct measurement of the corresponding lattice spacing change, averaged over the probed volume. Taking an aluminum (311) lattice plane spacing of 1.22 Å, the maximum displacement at about 5 ps after excitation corresponds to a (311) lattice space change of approximately 70 fm. The 0.02% sensitivity for the relative Bragg peak shift gives a detection limit of the lattice spacing change of less than 1 mÅ on the ultrafast time scale with FED.

The correlation between the in-plane Bragg peak motions observed with FED and the actual breathing motion of the Al film along the surface normal can be explained by the following picture. The film surface normal defines the directions for both laser-induced film breathing motion and the probe electron beam. The diffracting Bragg planes are the lattice planes forming the Bragg angle (θ) with the surface normal. The breathing motion of the film in the form of a 1-D standing wave creates an uneven stretch and compression to the film along the surface normal; that is, the atoms at the center of the film remain stationary, while the atoms at the two open surfaces experience the biggest vibration. This uneven stretching rotates the lattice planes toward the surface normal, which broadens the corresponding Bragg plane spacing accordingly and results in peak radius contraction. Similarly, uneven film compression will decrease the interplane spacing. In the diffraction pattern, this periodic film breathing motion will be exhibited as an oscillation of the Bragg ring radius for the polycrystal films as observed in FED.

At the relative low excitation power used in the current experiment, power-dependent measurements show the vibration amplitude to be proportional to the excitation laser fluence with no observable change of the vibrational period. This makes it possible to control the lattice dynamics with a sequence of pulses

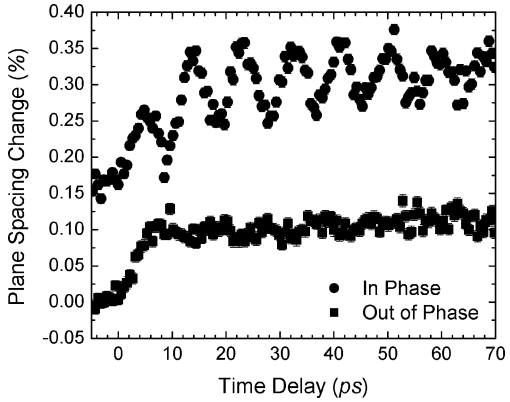

Figure 3. Coherent control of lattice vibrations using a pair of excitation laser pulses. The upper curve corresponds to the in-phase condition, where the time delay between the two pulses is equal to one vibrational period. The lower curve corresponds to the out-of-phase condition, with a time delay of one-half of the vibrational period.

by adjusting their relative intensities and time delays. Following the time-domain two-pathway-interference approach,[2,14,26] a Michelson interferometer was set in the laser path leading up to the sample to generate two excitation laser pulses separated by a well-defined time delay. In the interferometer, each incoming optical pulse was divided into two equal parts by a 50−50% beam splitter, and their time delay after exiting the interferometer was adjusted by changing the length difference between the two arms. Additionally, a quarter-wave plate was added in one arm and used in combination with a polarized beam splitter after the interferometer for controlling the energy ratio between the two beams.

The coherent lattice motions generated with the two-pulse excitation scheme are shown in Figure 3. By setting the time delay between the two optical pulses equal to one vibrational period, constructive interference was created between the two acoustic waves in the film. Compared with the single pulse data in Figure 2, the vibrational amplitude was nearly doubled at a given time delay, indicating in-phase constructive interference. In contrast, by setting the time delay equal to one-half of the vibrational period and the second pulse energy equal to approximately 92% of the first pulse to match the amplitudes of the two acoustic waves at a half vibrational period, the lattice vibration was completely silenced due to out-of-phase destructive interference. In this out-of-phase condition, the lattice was driven to a new equilibrium position within 10 ps. This ability to steer the lattice to a new equilibrium position in less than 10 ps can be used for ultrafast optical switching, such as slicing a portion of X-ray pulse generated at synchrotrons, which was recently demonstrated on the 100-ps time scale.[27]

In summary, the coherent lattice vibrations excited with femtosecond optical pulses were directly probed using femtosecond electron diffraction with sub-milli-angstrom spatial resolution and on the sub-picosecond time scale. Using a sequence of excitation pulses, we demonstrated the successful control of coherent lattice motions in less than 10 ps. These observations show that FED now has the potential to be used as a time-domain phonon spectroscopy tool for investigating the interaction of phonons with electronic and other excitations in solid materials, where coherent phonons, optical or acoustic, can be generated via impulsive optical excitation.

Acknowledgment. We would like to acknowledge the contributions of Dr. Zhao Hao in developing the femtosecond electron diffraction, the helpful discussions with Dr. H. Maris, and the funding from the National Science Foundation by Grant No. DMR-0305519.

References and Notes

(1) Warren, W. S.; Rabitz, H.; Dahleh, M. *Science* **1993**, *259*, 1581−1589.
(2) Tannor, D. J.; Rice, S. A. *J. Chem. Phys.* **1985**, *83*, 5013−5018.
(3) Weiner, A. M.; Leaird, D. E.; Wiederrecht, G. P.; Nelson, K. A. *Science* **1990**, *247*, 1317−1319.
(4) Hase, M.; Mizoguchi, K.; Harima, H.; Nakashima, S.; Tani, M.; Sakai, K.; Hangyo, M. *Appl. Phys. Lett.* **1996**, *69*, 2474−2476.
(5) Bartels, A.; Dekorsy, T.; Kurz, H.; Kohler, K. *Appl. Phys. Lett.* **1998**, *72*, 2844−2846.
(6) Sun, C. K.; Huang, Y. K.; Liang, J. C.; Abare, A.; DenBaars, S. P. *Appl. Phys. Lett*. **2001**, *78*, 1201−1203.
(7) Ozgur, U.; Lee, C. W.; Everitt, H. O. *Phys. Rev. Lett.* **2001**, *86*, 5604−5607.
(8) Lindenberg, A. M.; Kang, I.; Johnson, S. L.; Missalla, T.; Heimann, P. A.; Chang, Z.; Larsson, J.; Bucksbaum, P. H.; Kapteyn, H. C.; Padmore, H. A.; Lee, R. W.; Wark, J. S.; Falcone, R. W. *Phys. Rev. Lett.* **2000**, *84*, 111−114.
(9) Cavalleri, A.; Siders, C. W.; Brown, F. L. H.; Leitner, D. M.; Toth, C.; Squier, J. A.; Barty, C. P. J.; Wilson, K. R.; Sokolowski-Tinten, K.; von Hoegen, M. H.; von der Linde, D.; Kammler, M. *Phys. Rev. Lett.* **2000**, *85*, 586−589.
(10) Sokolowski-Tinten, K.; Blome, C.; Blums, J.; Cavalleri, A.; Dietrich, C.; Tarasevitch, A.; Uschmann, I.; Forster, E.; Kammler, M.; Horn-von-Hoegen, M.; von der Linde, D. *Nature* **2003**, *422*, 287−289.
(11) Cao, J.; Hao, Z.; Park, H.; Tao, C.; Kau, D.; Blaszczyk, L. *Appl. Phys. Lett.* **2003**, *83*, 1044−1046.
(12) Ruan, C. Y.; Lobastov, V. A.; Vigliotti, F.; Chen, S. Y.; Zewail, A. H. *Science* **2004**, *304*, 80−84.
(13) Siwick, B. J.; Dwyer, J. R.; Jordan, R. E.; Miller, R. J. D. *Science* **2003**, *302*, 1382−1385.
(14) Lindenberg, A. M.; Kang, I.; Johnson, S. L.; Falcone, R. W.; Heimann, P. A.; Chang, Z.; Lee, R. W.; Wark, J. S. *Opt. Lett.* **2002**, *27*, 869−871.
(15) Tas, G.; Maris, H. J. *Phys. Rev. B* **1994**, *49*, 15046−15054.
(16) Palik, E. D. *Handbook of optical constants of solids*; Academic Press: Orlando, FL, 1985.
(17) Zeiger, H. J.; Vidal, J.; Cheng, T. K.; Ippen, E. P.; Dresselhaus, G.; Dresselhaus, M. S. *Phys. Rev. B* **1992**, *45*, 768−778.
(18) Lide, D. R., Ed. *CRC Handbook of Chemistry and Physics*, 82nd ed.; Chemical Rubber Company: Boca Raton, FL, 2001−2002.
(19) Thomsen, C.; Strait, J.; Vardeny, Z.; Maris, H. J.; Tauc, J.; Hauser, J. J. *Phys. Rev. Lett.* **1984**, *53*, 989−992.
(20) Nisoli, M.; DeSilvestri, S.; Cavalleri, A.; Malvezzi, A. M.; Stella, A.; Lanzani, G.; Cheyssac, P.; Kofman, R. *Phys. Rev. B* **1997**, *55*, 13424−13427.
(21) Krauss, T. D.; Wise, F. W. *Phys. Rev. Lett.* **1997**, *79*, 5102−5105.
(22) Hartland, G. V. *J. Chem. Phys.* **2002**, *116*, 8048−8055.
(23) Williamson, J. C.; Zewail, A. H. *Chem. Phys. Lett.* **1993**, *209*, 10−16.
(24) Hodak, J. H.; Henglein, A.; Hartland, G. V. *J. Chem. Phys.* **1999**, *111*, 8613−8621.
(25) Thomsen, C.; Grahn, H. T.; Maris, H. J.; Tauc, J. *Phys. Rev. B* **1986**, *34*, 4129−4138.
(26) Potter, E. D.; Herek, J. L.; Pedersen, S.; Liu, Q.; Zewail, A. H. *Nature* **1992**, *355*, 66−68.
(27) DeCamp, M. F.; Reis, D. A.; Bucksbaum, P. H.; Adams, B.; Caraher, J. M.; Clarke, R.; Conover, C. W. S.; Dufresne, E. M.; Merlin, R.; Stoica, V.; Wahlstrand, J. K. *Nature* **2001**, *413*, 825−828.